Gas transport properties of adamantane-based polysulfones

M. R. Pixton and D. R. Paul*
*Department of Chemical Engineering and Center for Polymer Research,
The University of Texas at Austin, Austin, TX 78712, USA*
(Received 13 January 1995)

Gas transport of helium, hydrogen, oxygen, nitrogen, methane and carbon dioxide gases in 2,2-(4-hydroxy-phenyl)adamantane polysulfone and 1,3-(4-hydroxyphenyl)adamantane polysulfone has been measured. The adamantane-containing polymers have higher gas permeabilities in all cases and higher permselec-tivities in some cases compared with bisphenol A-based polysulfone (PSF). Oxygen solubility is higher for both adamantane-based polysulfones, particularly for the 2,2-isomer, and the high oxygen solubility coefficients are entirely responsible for the higher oxygen permeabilities compared with PSF. The physical properties of these materials are similar to those of fluorene bisphenol polysulfone (FBPSF); however, the T_g of the 2,2-isomer is higher while that of the 1,3-isomer is lower.

(Keywords: gas permeation; polysulfone; adamantane)

INTRODUCTION

Polysulfones have attracted significant interest as gas separation membrane materials owing to their combination of good physical and transport properties, chemical resistance and ease of synthesis. Numerous studies have described structure–gas transport property relationships and correlations in these materials[1-6]. In general, structural modifications that increase permeability also cause losses in permselectivity. This well known 'trade-off' relationship has been described in the literature[4,6]. Materials exceeding the typical trade-off curve have been produced by skilful design of the polymer molecular structure; however, an empirical 'upper-bound' relationship between selectivity and permeability has been proposed by Robeson above which no materials are currently known to exist[7].

Several general rules for the design of improved gas separation membrane materials have been identified[6,8]. Increased polymer fractional free volume (*FFV*) generally increases gas permeability, while inhibition of polymer chain rotational and flexural mobility generally increases permselectivity. Flexural mobility can be controlled by incorporating highly rigid, usually aromatic, segments into the polymer backbone and by limiting the number of flexible linkages in the repeat unit. Rotational mobility can be controlled by substitution of small groups onto the rotating units or through greater molecular asymmetry along the rotational axis. A general hypothesis is that both high permeability and high selectivity can be obtained simultaneously by generating an optimal distribution of polymer free volume. It has been proposed that a favourable free-volume distribution can be achieved by designing

polymer chains containing segments that cannot pack efficiently in alternating sequence with segments that can[9]. The repeat-unit structure of polysulfones, which consists of alternating bisphenol and sulfone monomer units, provides an excellent opportunity to test this hypothesis. Substitution on the bisphenol phenyl rings or changes in the bisphenol connector group can inhibit close chain packing and increase polysulfone *FFV*[1,2,4-6]. Owing to the requirements of the polymer synthesis, substitution of the sulfone monomer is usually not practicable.

The current study focuses on two adamantane-containing polysulfones. The alternation of long, flat sulfone units with packing-disruptive adamantyl groups should improve gas transport properties relative to other polysulfones with a less ordered structural variation. Numerous polymers containing adamantane, either as a pendent group or in the polymer backbone, have been reported in the literature[10-14]. In general, these materials have much higher thermal resistance than their aliphatic analogues. It is hoped that adamantane-containing polysulfones will also have superior membrane properties as compared with the current generation of polysulfone gas separation materials.

EXPERIMENTAL

The sources of the monomers and their purification are briefly described in *Table 1*. 2-Adamantanone and phenol were condensed in the presence of hydrogen chloride and thiolactic acid to give 2,2-(4-hydroxy-phenyl)adamantane (2,2-ADM)[12,15]. 1,3-(4-Hydroxy-phenyl)adamantane (1,3-ADM) was synthesized from 1,3-dibromoadamantane and phenol according to a literature procedure[14]. The appropriate bisphenol and 4-fluorophenyl sulfone (4-FPS), dissolved in toluene

---

and *N*-methylpyrrolidinone (NMP), were condensed in the presence of reagent-grade potassium carbonate to give the polysulfone following the procedure of Mohanty[16] as modified by McHattie[4]. Each polymer was precipitated from solution into ethanol and then extracted with ethanol for 48 h in a Soxhlet apparatus to remove any residual NMP solvent. The intrinsic viscosity for each polymer in chloroform at 25°C was measured using a size 25 Cannon-Fenske capillary viscometer as an indication of molecular weight. The polymer structures and their name abbreviations are listed in *Table 2*. Data for a number of polysulfones and polycarbonates tested previously are included for comparison[3,4,17].

Polymer films 2–3 mil ($\sim$50–75 μm) in thickness were cast onto glass plates from approximately 5 wt% chloroform solutions. After most of the solvent had evaporated, the clear films were stripped from the glass plates and vacuum dried, first at room temperature for 24 h and then at incrementally higher temperatures until 150°C was reached after about 4 days. The films were held above 150°C for at least 24 h and then removed from the vacuum oven. Thermogravimetric analysis (t.g.a.) using a Perkin-Elmer TGA-7 verified complete solvent removal from the vacuum-dried films.

The glass transition temperature (T_g) of each polymer was measured using a Perkin-Elmer DSC-7 differential scanning calorimeter (d.s.c.) at a heating rate of 20°C min^{-1}. The samples were heated twice and the T_g was taken as the midpoint of the transition during the second scan. It was concluded that both polysulfones are amorphous since no crystalline melting points were observed. Dynamic mechanical analysis (d.m.a.) was performed using a Polymer Laboratories DMTA operated at a frequency of 3 Hz from -150 to 200°C at a heating rate of 4°C min^{-1}. Several strips of film were laminated together in a small press, at 15 to 20°C above the polymer T_g, for 5 min to form a small test bar ($\sim$1.5 mm in thickness) for d.m.a. The polymer bars were rapidly quenched to room temperature after pressing to standardize the thermal history of each sample.

Wide-angle X-ray diffraction (WAXD) scans were made for each polymer using a Phillips APD 3520 X-ray diffractometer at a Cu Kα wavelength of 1.54 Å. The broad peak obtained for amorphous polymers can be an indicator of the average chain spacing. The corresponding *d*-spacings were calculated from the diffraction peak maxima using the Bragg equation, $n\lambda = 2d \sin \theta$. Polymer densities were measured in a density gradient column based on degassed, aqueous solutions of calcium nitrate at 30°C. The polymer density was used to calculate its fractional free volume (*FFV*) following the method of Bondi and van Krevelen[18,19]:

$$FFV = (V - V_0)/V \tag{1}$$

where V is the measured polymer specific volume and V_0 is the occupied volume. The occupied volume can be estimated from the van der Waals volume (V_W) according to the relation:

$$V_0 = 1.3 V_W \tag{2}$$

The factor of 1.3 is only approximate and is estimated from data for only a few polymeric materials. Quantitative evaluation of *FFV* is difficult; however, qualitative and semi-quantitative comparisons between materials with similar structures have proven useful. The van der

Waals volume of the 2,2-adamantyl group was calculated as 77.78 cm^3 mol^{-1} while that of the 1,3-adamantyl group was calculated as 77.71 cm^3 mol^{-1} based on Bondi's data.

Pure gas permeability coefficients at 35°C for He, H$_2$, O$_2$, N$_2$, CH$_4$ and CO$_2$ gases were measured in a pressure-rise type of permeation cell using the standard technique employed in our laboratory[20]. All the gases were chromatography-grade, with the exception of CH$_4$, which was chemically pure grade. H$_2$ and O$_2$ permeabilities were measured up to 6 atm while He, N$_2$, CH$_4$ and CO$_2$ permeabilities were measured up to 20 atm upstream pressure. CO$_2$ permeation was measured last since time-dependent hysteresis has been observed for CO$_2$ pressurization and depressurization cycles in some materials[21,22]. Ideal permselectivities ($\alpha^*_{A/B}$) were calculated from:

$$\alpha^*_{A/B} = P_A/P_B \tag{3}$$

where P_A and P_B are the permeabilities of pure gases A and B. Assuming the absence of penetrant–penetrant interactions or plasticization, this ideal permselectivity provides a good estimate of actual mixed gas performance when the downstream pressure is negligible in comparison to the upstream pressure. Pure gas sorption of O$_2$ at pressures up to 6 atm and N$_2$, CH$_4$ and CO$_2$ at pressures up to 35 atm was measured in a two-volume pressure decay type of sorption cell at 35°C[23,24].
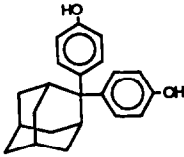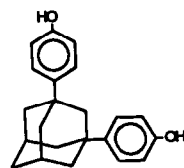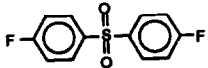
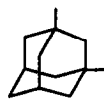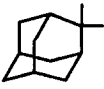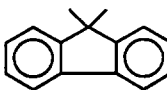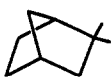## POLYMER CHARACTERIZATION

Physical properties

The T_g of 2,2-ADM PSF is 55°C higher than that of 1,3-ADM PSF (see *Table 2*). Differences in barriers to molecular motion apparently are responsible for this rather substantial difference in T_g. The bisphenol phenyl rings of the 1,3-isomer are relatively free to rotate around the bond axes, while those of the 2,2-isomer are constrained in their relative position and rotational freedom by steric interactions. Additionally, the polymer chain based on the 2,2-isomer is more 'kinked' than for the 1,3-isomer because the phenyl rings are connected to the same carbon atom. Both effects influence the T_g of these polymers. The T_g of 2,2-ADM PSF is over 100°C higher than that of the polysulfone based on bisphenol A (PSF) and 20°C higher than that of the polysulfone based on 9,9-(4-hydroxyphenyl)fluorene (FBPSF). This last comparison is of particular interest as the fluorenylidene connector group is quite rigid and has a higher molecular mass than the 2,2-adamantylidene connector group. A previous study showed that the bicyclic bisphenol connector in the polycarbonate based on 4,4-(4-hydroxy-phenyl)norbornane (NBPC) greatly increased the T_g relative to the polycarbonate based on bisphenol A (PC)[17]. The presence of a rigid, multicyclic bisphenol connector group appears to produce the same effect in polysulfones.

The observed *d*-spacings and densities for these polymers are listed in *Table 2*. The *d*-spacing of 2,2-ADM PSF is larger than that of 1,3-ADM PSF, while both materials have larger *d*-spacings than the other two polysulfones shown. 1,3-ADM PSF is slightly more dense than 2,2-ADM PSF, which corresponds well with the *d*-spacing results. The calculated fractional free

Table 1 Monomer sources and purification

Monomer	Abbreviation	Source	Purification	Melting point (°C)[a]
	2,2-ADM	Synthesis	Sublimation	316–318
	1,3-ADM	Synthesis	Recrystallization	200–202
	4-FPS	Aldrich	Sublimation	99–100

[a] After purification

Table 2 Polysulfone and polycarbonate structures and physical properties

R₁	Polymer abbreviation	T_g (°C)	T_{γ_1} (°C)	T_{γ_2} (°C)	ρ (g cm^{-3})	d-spacing (Å)	FFV^c	$[\eta]^d$ (dl g^{-1})
Polysulfones								
	1,3-ADM PSF	242	–	−90	1.238	5.1	0.153	0.80
	2,2-ADM PSF	297	–	−83	1.231	5.4	0.158	0.43
-C(CH₃)₂-	PSF^e	186	–	−80	1.240	5.0	0.156	0.40
	FBPSF^f	277	−30	−85	1.245	4.7	0.165	0.96
-C(CH₃)₂-	PC^g	150	–	−72	1.20	5.2	0.164	–
Polycarbonates	NBPC^g	235	–	−75	1.20	5.1	0.174	0.55

[a] The general polysulfone structure is
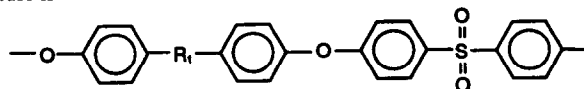
[b] The general polycarbonate structure is
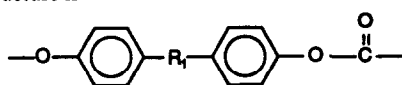
[c] FFV calculated using method of Bondi
[d] At 25°C in chloroform
[e] Data from ref. 4
[f] Data from ref. 3
[g] Data from ref. 17

volume of 1,3-ADM PSF is slightly lower than that of 2,2-ADM PSF (see *Table 2*). The greater number of conformational constraints in 2,2-ADM PSF is most likely responsible for the differences in physical properties of these two polysulfones based on isomers of adamantane bisphenol.

The dynamic mechanical spectra of polysulfones show various relaxation processes, which are usually labelled α, β and γ, going down the temperature scale. The α relaxation indicates the onset of large-scale chain motions characteristic of the glass transition. The β peak appears to represent relaxations of non-equilibrium packing defects in the glass or of stresses introduced during fabrication[25,26], and can be reduced or eliminated by sub-T_g annealing. The γ relaxation is believed to indicate the onset of molecular motion by individual units or small segments of the polymer backbone. In polycarbonates, cooperative motions of several adjacent monomer units appear to be involved[27]. In polysulfones, however, the γ relaxation appears to involve uncoupled motions of the individual monomer units. This difference has been attributed to the greater flexibility of the polysulfone ether linkage as compared with a carbonate linkage. Past studies of polysulfones have shown that the γ relaxation can be separated into two components: γ_1 represents motions of the bisphenol unit and γ_2 represents motions of the diphenyl sulfone unit[28]. These two components are superimposed in many cases and thus only one γ peak is observed. The γ_2 relaxation temperature, T_{γ_2}, decreases with increasing *FFV* and has an asymptote at approximately $-100°C$. The γ_1 relaxation temperature, T_{γ_1}, increases sharply following bisphenol phenyl ring substitution or in the presence of a polar bisphenol connector group. This study will follow the convention established in previous work of labelling the γ peaks 1 and 2 going down the temperature scale. In those cases where only one peak appears, it will be labelled γ_2.

The d.m.t.a. traces for the adamantane-based polysulfones are shown in *Figure 1*; the temperatures at which the sub-T_g γ relaxations occur are summarized in *Table 2*. For both the adamantane-based polysulfones, there is only one broad tan δ peak observed in the γ region. The tan δ peak in the γ region for 1,3-ADM PSF is larger than the much broader peak for the 2,2-isomer. The γ_2 transition temperature for 1,3-ADM PSF is 7°C lower than that for 2,2-ADM PSF. Steric interactions between the two bisphenol phenyl rings, which increase intermolecular barriers to small-scale motion, may account for this difference and for the broadening of the 2,2-isomer tan δ peak. The γ_2 transition temperature of FBPSF is very close to that for the adamantane-based materials; however, the γ_1 peak noted for FBPSF near $-30°C$ was not observed here. It appears that the aromatic fluorenylidene connector group inhibits bisphenol monomer unit mobility in a manner not observed for the aliphatic connector groups in 2,2-ADM PSF, 1,3-ADM PSF and PSF where the γ_1 transition is probably superimposed on the γ_2 transition. *Figure 2* shows a plot of T_{γ_2} versus *FFV* for the adamantane-based materials plus a number of other polysulfones[1,2,4-6]. The current data correlate well with the results of previously tested polysulfones.

Permeation

Pure gas permeability coefficients and ideal
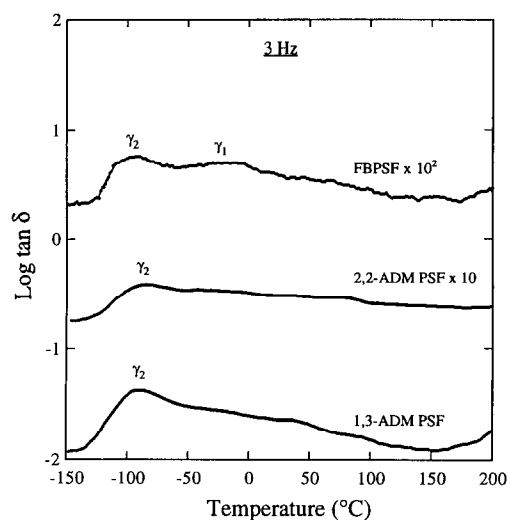
Figure 1 Log tan δ at 3 Hz as a function of temperature for the adamantane-based polysulfones. The curve for the 1,3-ADM PSF material corresponds to the tan δ scale shown, while the curve for 2,2-ADM PSF has been shifted upwards by a factor of 10 for clarity. The data for FBPSF, taken from ref. 3, are included for comparison
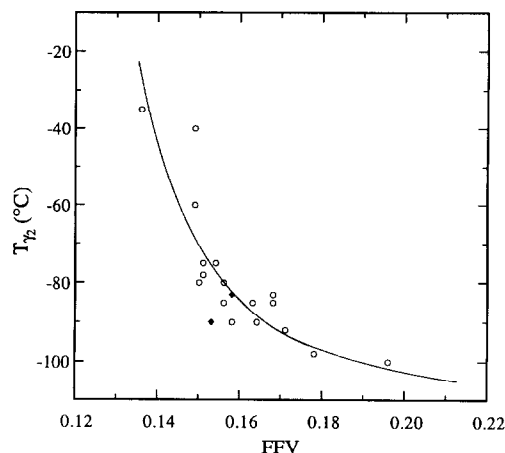
Figure 2 Relationship between the sub-T_g relaxation temperature T_{γ_2} and fractional free volume (*FFV*). Solid diamonds represent the adamantane-based polysulfone data while the open circles are for polysulfones described elsewhere. The full curve represents the best fit of the polysulfone data

Table 3 Helium permeability and ideal selectivities at 35°C

Polymer	P_{He} (10 atm) (barrer)[a]	α^*_{He/CH_4} (10 atm)	α^*_{He/H_2} (2 atm)
1,3-ADM PSF	13.8	41	0.80
2,2-ADM PSF	21.7	56	0.78
PSF[b]	13	49	0.93
FBPSF[c]	21.3	40	–
PC[d]	13	35	–
NBPC[d]	19	38	0.86

[a] Barrer = 10^{-10} cm cm^3(STP)/cm^2 s cmHg
[b] Data from ref. 4
[c] Data from ref. 3
[d] Data from ref. 17

Table 4 Mobility and solubility components of the O_2/N_2 separation factor[a]

| Polymer	P_{O_2} (barrer)	$\alpha^*_{O_2/N_2}$	$\bar{S}_{O_2}$ (cm^3(STP)cm^{-3} atm^{-1})	$\bar{S}_{O_2}/\bar{S}_{N_2}$	$\bar{D}_{O_2} \times 10^8$ (cm^2 s^{-1})	$\bar{D}_{O_2}/\bar{D}_{N_2}$
1,3-ADM PSF	1.86	5.6	0.37	1.8	3.8	3.1
2,2-ADM PSF	2.55	5.6	0.63	1.4	3.1	4.0
PSF[b]	1.4	5.6	0.24	1.6	4.4	3.6
FBPSF[c]	2.76	5.7	0.48	1.7	4.3	3.3
PC[d]	1.6	4.8	0.21	1.5	5.8	3.2
NBPC[d]	2.4	5.1	0.41	1.5	4.4	3.3

[a] Data at 35°C and 2 atm
[b] Data from ref. 4
[c] Data from ref. 3
[d] Data from ref. 17

Table 5 Mobility and solubility components of the CO_2/CH_2 separation factor[a]

| Polymer	P_{CO_2} (barrer)	α_{CO_2/CH_4}	$\bar{S}_{CO_2}$ (cm^3(STP)cm^{-3} atm^{-1})	$\bar{S}_{CO_2}/\bar{S}_{CH_4}$	$\bar{D}_{CO_2} \times 10^8$ (cm^2 s^{-1})	$\bar{D}_{CO_2}/\bar{D}_{CH_4}$
1,3-ADM PSF	7.2	22	2.0	3.2	2.8	6.7
2,2-ADM PSF	9.5	24	2.6	2.5	2.7	9.6
PSF[b]	5.6	22	2.1	3.7	2.0	5.9
FBPSF[c]	14	26	5.3	3.9	2.0	6.7
PC[d]	5.9	18	1.2	4.0	3.7	4.5
NBPC[d]	9.1	19	2.5	3.9	2.8	4.8

[a] Data at 35°C and 10 atm
[b] Data from ref. 4
[c] Data from ref. 3
[d] Data from ref. 17
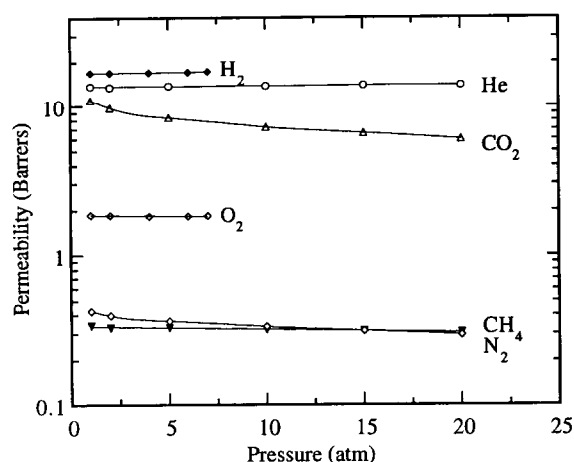
Figure 3 Pressure dependence of 1,3-ADM PSF permeability coefficients at 35°C
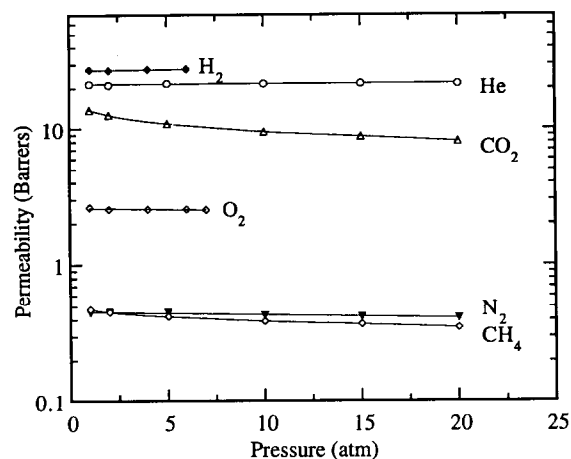
Figure 4 Pressure dependence of 2,2-ADM PSF permeability coefficients at 35°C

selectivities for gas pairs of particular interest are shown in *Tables 3–5*. Permeability isotherms at 35°C are given in *Figures 3* and *4* as a function of upstream driving pressure. The permeability coefficients for the larger penetrant molecules decrease with increasing upstream pressure as predicted by the frequently used dual-mode sorption model for glassy polymers. The permeability of 2,2-ADM PSF is approximately 35% higher than that of 1,3-ADM PSF for He, O_2 and CO_2. The selectivity of 2,2-ADM PSF for He/CH_4 and CO_2/CH_4 is higher than

that of 1,3-ADM PSF, while the two polysulfones show the same selectivity for O_2/N_2. Comparison of PC with NBPC shows that the presence of a rigid bicyclic connector group increases both permeability and selectivity for all of the gas pairs shown. A similar comparison of the current materials with PSF shows that the 2,2-isomer has a higher permeability and the same or a higher selectivity for all of the reported gas pairs except He/H_2, while the 1,3-isomer has higher permeability for all the gases and the same selectivity except for He/H_2
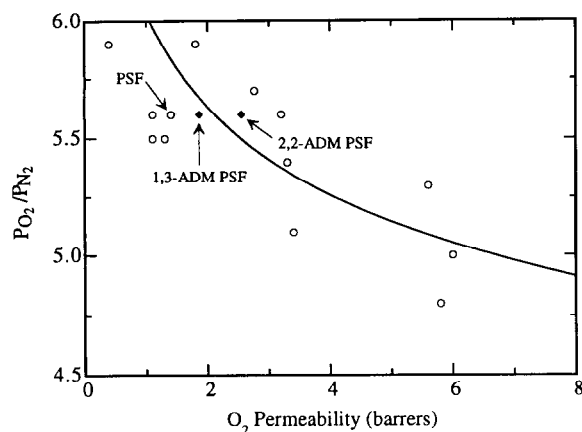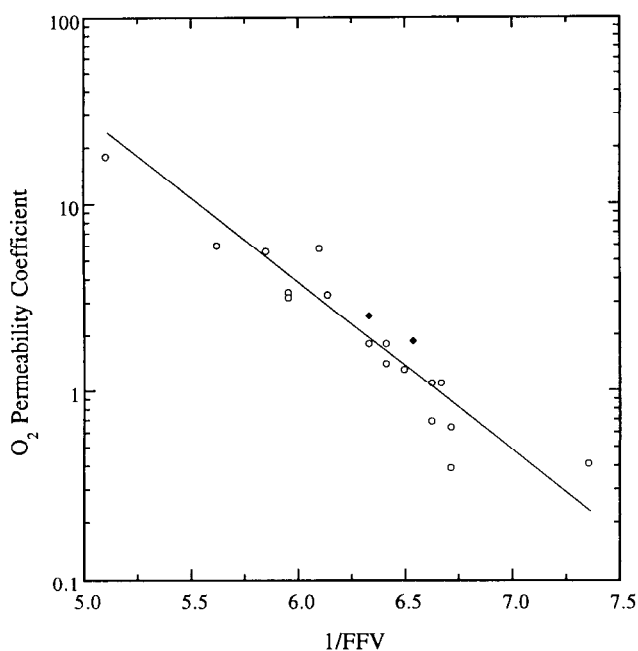
Figure 5 Relationship between O_2 permeability and O_2/N_2 selectivity for various polysulfones. Solid diamonds represent the adamantane-based polysulfone data while the open circles are for polysulfones described elsewhere. The full curve represents the best power-law fit for this set of polymers and illustrates the typical trade-off relationship for this group of materials
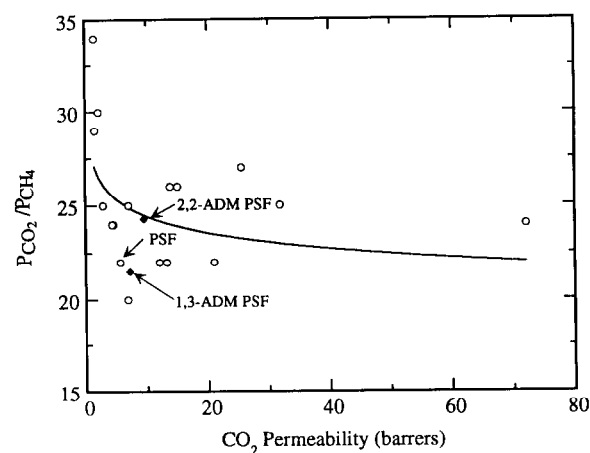

Figure 6 Relationship between CO_2 permeability and CO_2/CH_4 selectivity for various polysulfones. Solid diamonds represent the adamantane-based polysulfone data while the open circles are for polysulfones described elsewhere. The full curve represents the best power-law fit for this set of polymers and illustrates the typical trade-off relationship for this group of materials

Figure 7 Correlation of O_2 permeability with inverse fractional free volume. Solid diamonds represent the current polysulfone data while open circles correspond to various polysulfones described elsewhere. The line is the best linear fit to the latter data
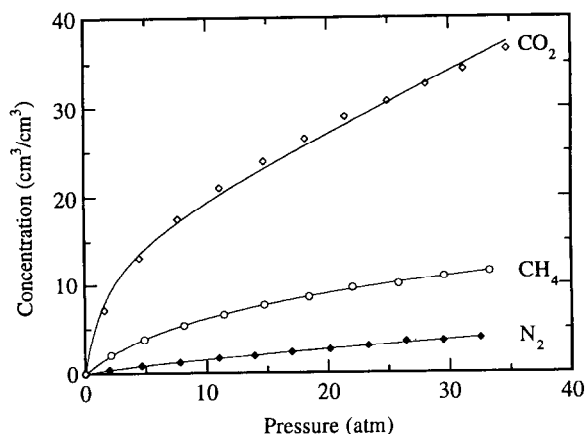
Figure 8 Sorption isotherms for N_2, CH_4 and CO_2 in 1,3-ADM PSF at 35°C

Figure 9 Sorption isotherms for N_2, CH_4 and CO_2 in 2,2-ADM PSF at 35°C

and He/CH_4. The magnitudes of the increases in permeability and selectivity are smaller for the adamantane-based polysulfones than observed for NBPC relative to PC; this no doubt relates to the much lower concentration of rigid multicyclic connector groups in the polysulfone repeat unit.
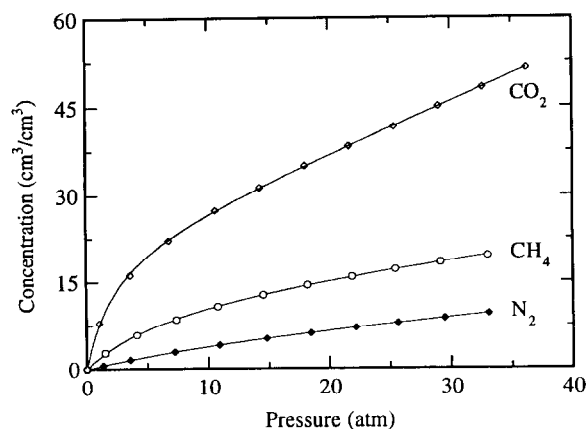
The relationship between permeability and selectivity is shown graphically in *Figure 5* for O_2/N_2 and *Figure 6* for CO_2/CH_4. The O_2/N_2 separation properties of the adamantane-containing polysulfones are typical of other polysulfones. Note that both materials are superior to PSF for O_2/N_2 separation, i.e. they both have the same O_2/N_2 selectivity but higher O_2 permeability than PSF. The CO_2/CH_4 separation properties of the adamantane-based materials are inferior to those of a number of other polysulfones. CO_2/CH_4 selectivity has been correlated with several factors including the polar group concentration of the material. As the adamantane-based polysulfones have a low polar group concentration, it is not surprising that the CO_2/CH_4 selectivities are unimpressive.

Theoretical studies have suggested and previous experimental results have confirmed a correlation between gas permeability P and fractional free volume FFV of the form[1,6]:

$$P = A \exp(-B/FFV) \tag{4}$$

where the parameters A and B depend on both gas and temperature but not on polymer type. A semilogarithmic plot of O_2 permeability *versus* inverse FFV is shown in *Figure 7* for these polyarylates along with data for a number of other polyarylates and polysulfones. As suggested by equation (4), the correlation of these data is quite good. More quantitative determination of FFV, perhaps by molecular modelling, might allow even better fitting of the data to the above equation.

Sorption

Pure gas sorption isotherms (35°C) for N_2, CH_4 and CO_2 are shown in *Figures 8* and *9* for these polysulfones. The level of gas sorption is usually correlated with gas condensibility; hence, CO_2 sorption is highest, followed by CH_4 and then N_2. The overall gas permeability P can be factorized into solubility and diffusivity terms according to:

$$P = \bar{D}\bar{S} \tag{5}$$

where $\bar{D}$ is the concentration-averaged diffusion coefficient and $\bar{S}$ is the solubility coefficient calculated from the secant slope of the sorption isotherm evaluated at the upstream condition. The ideal overall permselectivity (equation (3)) can be factored into solubility and diffusivity terms using equation (5) to give:

$$\alpha_{A/B}^* = \frac{P_A}{P_B} = \left(\frac{\bar{D}_A}{\bar{D}_B}\right)\left(\frac{\bar{S}_A}{\bar{S}_B}\right) \tag{6}$$

where $\bar{D}_A/\bar{D}_B$ is the diffusivity selectivity and $\bar{S}_A/\bar{S}_B$ is the solubility selectivity. The O_2 and CO_2 solubility and diffusivity coefficients as well as the calculated solubility and diffusivity selectivities for the gas pairs O_2/N_2 and CO_2/CH_4 of these materials are compared in *Tables 4* and *5*. Compared to 1,3-ADM PSF, the O_2 solubility and O_2/N_2 diffusivity selectivity are higher, while the O_2 diffusivity and O_2/N_2 solubility selectivity are lower for 2,2-ADM PSF. The absolute levels of O_2 solubility are higher while the O_2 diffusivities are lower for the adamantane-based polysulfones than for PSF. The higher O_2 permeability of the adamantane-based materials, as compared with PSF, is due entirely to their higher O_2 solubility. Similarly, the level of O_2 solubility is much higher but the diffusivity is lower for NBPC than for PC. For CO_2, solubility is higher in the 2,2-ADM PSF isomer but CO_2/CH_4 solubility selectivity is lower than for 1,3-ADM PSF.

The effect of FFV on the gas sorption capacity S is shown in *Figure 10* for O_2 (2 atm) and in *Figure 11* for CO_2 (10 atm). For O_2, the 2,2-ADM PSF value falls slightly outside the band, defined by the two dashed lines in *Figure 10*, occupied by a large number of other polysulfones including 1,3-ADM PSF. For CO_2, both adamantane-based polysulfone values fall within a similar band containing the polysulfone data. The high gas sorption of the 2,2-isomer is not well understood;
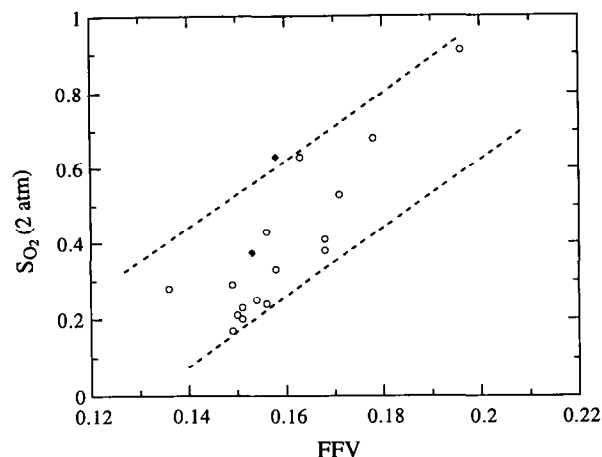
Figure 10 Correlation of the O_2 solubility coefficient (2 atm) at 35°C with fractional free volume. Diamonds represent the adamantane-based polysulfones described here while open circles correspond to various polysulfones described elsewhere. The dashed lines represent the approximate boundaries of the polysulfone data
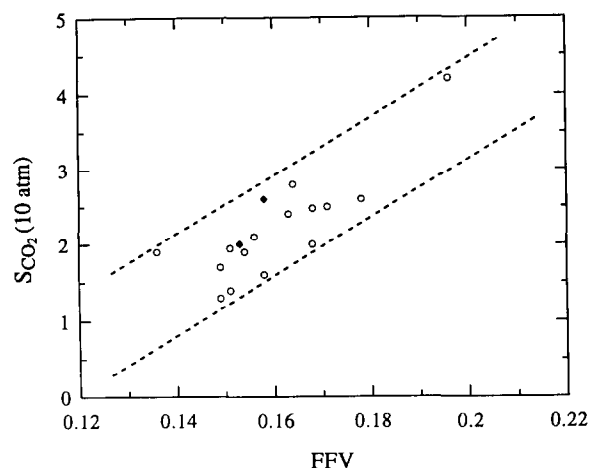
Figure 11 Correlation of the CO_2 solubility coefficient (10 atm) at 35°C with fractional free volume. Diamonds represent the adamantane-based polysulfones described here while open circles correspond to various polysulfones described elsewhere. The dashed lines represent the approximate boundaries of the polysulfone data

however, it is consistent with the high gas sorption of NBPC as mentioned previously.

The sorption data can be well described by the dual-mode sorption model[29,30]:

$$C = k_D p + \frac{C'_H bp}{1 + bp} \tag{7}$$

where k_D is the Henry's law solubility coefficient, C'_H is the Langmuir capacity factor and b is an affinity parameter characterizing the relative rates of sorption and desorption. Non-linear curve fitting of the sorption data to the dual-mode sorption model using the Levenberg–Marquardt algorithm allows calculation of all three model parameters for the gases N_2, CH_4 and CO_2 (see *Table 6*).

CONCLUSIONS

The gas sorption and transport properties of 1,3-ADM

Table 6 Dual-mode sorption parameters at 35°C

Polymer	Gas	k_D (cm³(STP)/cm³ atm)	C'_H (cm³(STP)/cm³)	b (atm⁻¹)
1,3-ADM PSF	N_2	0.100	0.93	0.142
	CH_4	0.102	10.76	0.093
	CO_2	0.565	19.25	0.289
2,2-ADM PSF	N_2	0.209	3.48	0.111
	CH_4	0.245	14.18	0.129
	CO_2	0.841	22.28	0.430

PSF and 2,2-ADM PSF have been described. The adamantane connector group increases the gas permeability in all cases and the permselectivity in some cases compared with bisphenol A-based polysulfone (PSF). Oxygen sorption is significantly higher for both adamantane-based polysulfones than for PSF, particularly for the 2,2-isomer, and higher O_2 solubility coefficients are entirely responsible for the higher O_2 permeabilities. The 2,2-adamantylidene connector group appears to stiffen the polymer chain even more significantly than the fluorenylidene connector group, as indicated by the glass transition temperatures.

ACKNOWLEDGEMENTS

REFERENCES

1   Aitken, C. L., Koros, W. J. and Paul, D. R. *Macromolecules* 1992, **25**, 3424
2   Aitken, C. L., Koros, W. J. and Paul, D. R. *Macromolecules* 1992, **25**, 3651
3   Aguilar-Vega, M. and Paul, D. R. *J. Polym. Sci., Polym. Phys. Edn.* 1993, **31**, 1599
4   McHattie, J. S., Koros, W. J. and Paul, D. R. *Polymer* 1991, **32**, 840
5   McHattie, J. S., Koros, W. J. and Paul, D. R. *Polymer* 1991, **32**, 2618
6   McHattie, J. S., Koros, W. J. and Paul, D. R. *Polymer* 1992, **33**, 1701
7   Robeson, L. M. *J. Membr. Sci.* 1991, **62**, 165
8   Koros, W. J., Story, B. J., Jordan, S. M., O'Brien, K. and Husk, G. R. *Polym. Eng. Sci.* 1987, **27**, 603
9   Pessan, L. A., Ph.D. Dissertation, The University of Texas at Austin, 1993
10   Archibald, T. G., Malik, A. A. and Baum, K. *Macromolecules* 1991, **24**, 5261
11   Bellmann, G. and Tao, N. V., US Patent 4332964, 1982
12   Papava, G. S., Beridze, L. A., Gelshvili, N. S. and Tsiskarishvili, P. D. *Izv. Akad. Nauk Gruz. SSR, Ser. Khim.* 1975, **1**, 235
13   Thompson, R. M. and Duling, I. N., US Patent 3738960, 1973
14   Moore, R. E. and Duling, I. N., US Patent 3516968, 1970
15   Lerman, B. M., Aref'eva, Z. Y., Galin, F. Z. and Tolstikov, G. A. *Izv. Akad. Nauk SSSR, Ser. Khim.* 1974, **3**, 720
16   Mohanty, D. K., Ph.D. Dissertation, Virginia Polytechnic Institute and State University, 1983
17   McHattie, J. S., Koros, W. J. and Paul, D. R. *J. Polym. Sci., Polym. Phys. Edn.* 1991, **29**, 731
18   Bondi, A. 'Physical Properties of Molecular Crystals, Liquids, and Glasses', Wiley, New York, 1968
19   Van Krevelen, D. W. 'Properties of Polymers', 3rd Edn., Elsevier Science, New York, 1990
20   Koros, W. J., Paul, D. R. and Rocha, A. A. *J. Polym. Sci. Polym. Phys. Edn.* 1976, **14**, 687
21   Jordan, S. M., Koros, W. J. and Fleming, G. K. *J. Membr. Sci.* 1987, **30**, 191
22   Raymond, P. C. and Paul, D. R. *J. Polym. Sci., Polym. Phys. Edn.* 1990, **28**, 2213
23   Koros, W. J., Chan, A. H. and Paul, D. R. *J. Membr. Sci.* 1977, **2**, 165
24   Koros, W. J. and Paul, D. R. *J. Polym. Sci., Polym. Phys. Edn.* 1976, **14**, 1903
25   Illers, K. H. and Breuer, H. *J. Colloid Sci.* 1963, **18**, 1
26   Yee, A. F. and Smith, S. A. *Macromolecules* 1981, **14**, 54
27   Jho, J. Y. and Yee, A. F. *Macromolecules* 1991, **24**, 1905
28   Aitken, C. L., McHattie, J. S. and Paul, D. R. *Macromolecules* 1992, **25**, 2910
29   Vieth, W. R., Howell, J. M. and Hsieh, J. H. *J. Membr. Sci.* 1976, **1**, 177
30   Barrer, R. M., Barrie, J. A. and Slater, J. *J. Polym. Sci.* 1958, **27**, 177